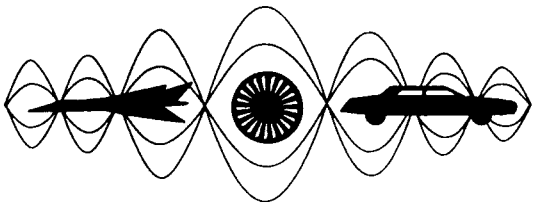

FIFTH INTERNATIONAL CONGRESS ON SOUND AND VIBRATION
DECEMBER 15-18, 1997
ADELAIDE, SOUTH AUSTRALIA

MODELING OF ELECTRO-MAGNETIC EXCITATION FORCES OF AN INDUCTION MOTOR FOR VIBRATION AND NOISE ANALYSIS

Dae-Hyeon Cho* and Kwang-Joon Kim**

*Samsung Aerospace Industries, Ltd, Korea
**Center for Noise and Vibration, Dept. of Mechanical Engineering, KAIST , Korea

ABSTRACT

Electric motors are the most fundamental source of motion generation mechanisms in both industrial and household products. Noise and vibration problems in such products can be remedied in general at each of the three stages ; source-transmission path-receiver. Some problems, however, caused inherently by the motors can not be successfully resolved by working on the transmission path or the receiver alone. In this regard, importance of the noise and vibration problems in the motor itself has been increasing so far.

In this paper, a method is presented, which can calculate electromagnetic forces in quantitative as well as qualitative aspects, based on equivalent transformer circuit. Here the rotor slot skew, permeance fluctuations and rotor dynamics are also taken into consideration. Even though this method does not yield information so detailed as the FEM, the computational burden is very low. By using this method, distributions of the electromagnetic forces in both spatial and temporal frequency domain are investigated and effects of the rotor eccentricity and rotor-slot-opening are also investigated. The reason why the exciting force increases and consequently the noise level goes up in reality with loading is explained. Finally, results of the simulation are compared with the experiments.

1. INTRODUCTION

In the experimental research on noise and vibration of induction motors so far, vibrations are measured on the surface of the motor frame together with sound pressure levels around the motor and then the measurements are analyzed in connection with modal properties of the motor structure and electromagnetic excitation mechanisms[1-2]. In the analytical works, estimation of Maxwell stress acting on the stator due to magnetic flux in the air gap is the major concern. The Maxwell stress can be estimated by using the classical magneto-motive force and permeance wave theory[3], according to which peak frequencies in

the power spectrum of the Maxwell stress can be easily located even though magnitudes of the peaks are not well predicted. Detailed distribution of the flux density in the air gap can be calculated by using the finite element method(FEM)[4]. Although this method yields the qualitative as well as quantitative characteristics of the Maxwell stress, computational burden is rather high.

In this paper, a method[5] to calculate the electromagnetic forces based on the equivalent transformer circuits[6] is proposed, which is far simple compared with the FEM but still capable of estimating the excitation forces in the qualitative as well as quantitative aspects by taking into consideration the effects of rotor slot skew and permeance fluctuations due to the rotor rotation. Even though this method may not yield information as detailed as the FEM, the computational burden is very low. By using this method, distributions of the electromagnetic forces are investigated in both spatial frequency and temporal frequency domain, and effects of the rotor eccentricity and rotor-slot-opening are investigated. Then, some of the simulation results are confirmed by experimentation. Specifications of the induction motor under investigation are shown in Tables 1 and 2.

Table 1. Electrical spec. of induction motor under investigation

Specification		Value	Unit
Voltage source	Number of phase	3	
	Phase voltage(V)	220	V(rms)
	Frequency(f_p)	60	Hz
Poles	Number(p)	4	
Nominal output	Horse power	5	Hp
Rotor type		Squirrel cage	

Table 2. Mechanical spec. of induction motor under investigation

Specification		Value	Unit
Rotor speed	Rated rpm(60×n)	1730	rpm
Stator slot	Number(z_S)	48	
Rotor slot	Number(z_R)	40	
	Skew	5.3	degree
Length	Stack height (h)	0.085	meters
Air gap	Inner radius (r)	0.06	meters
	Distance (d_O)	0.0003	meters

2. Estimation of the electromagnetic excitation forces

The electromagnetic circuit of the induction motor is modeled in this paper by the classical transformer model, where the current in the stator is composed of one for the magnetization and another for the load and the flux change due to rotor current is canceled out by that due to the current induced subsequently in the stator. More considerations are added to the classical transformer model here ; 1) inductance of the stator coil is divided into as many parts as the number of the stator teeth in order to calculate the electromagnetic excitation force at each stator tooth, which means that smooth sinusoidally-distributed winding patterns are not assumed any more, and 2) skew of the rotor slot and fluctuation of the permeance caused by the rotor rotations are taken into account.

2.1 Analytical modeling of electro-mechanical characteristics of a 3-phase squirrel cage induction motor

The magnetic flux in the air gap, which is responsible for the electromagnetic excitation force, is generated by the magneto motive forces, i.e., currents in the stator coils and rotor conductors. In induction motors, these currents are determined by the terminal voltage, induced voltage, resistance of electric circuit, reluctance of magnetic circuit, and slip. Several assumptions are made in order to derive simplified relations among them as follows :
1) All fluxes coming out of a stator tooth enter the rotor and link the rotor conducting bars as shown in Fig. 1(a). This applies also to the fluxes from a rotor teeth. That is, no flux

leakage occurs.

2) The fluxes due to the current in a bundle of stator coils wound around multiple teeth are equal to the summation of those due to the same bundle of coils wound around each single tooth(See Fig. 1(a))[7].

3) The detailed shape of the slot is not taken into account. Instead, it is represented in terms of equivalent width of the slot opening. Fluxes in the air gap are completely in the radial direction and, hence, eccentricity of the rotor is reflected in terms of spatial variation of the reluctance around the stator(or rotor).

4) Because permeability of the core material is much higher than the air, reluctance of the core is neglected.

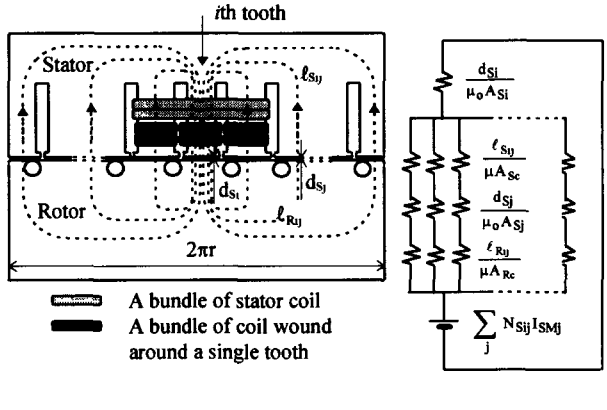

(a) (b)

Fig. 1 Magnetic fluxes due to stator current

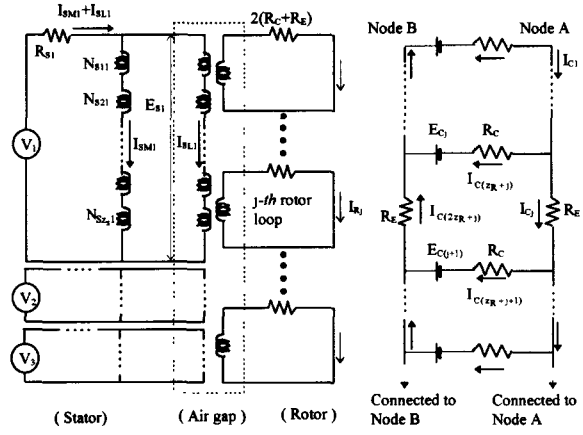

(a) (b)

Fig. 2 Electromagnetic circuit of induction motor based on transformer circuit

Now, consider a bundle of coils wound around a single stator tooth as shown in Fig. 1(a). Reluctance of the magnetic path, Q_{Si}, through the i-*th* stator tooth can be obtained using an equivalent circuit as shown in Fig. 1(b) and 4-*th* assumption. Introducing a diagonal matrix $\mathbf{Q}_S = \mathrm{Diag}(Q_{S1}, Q_{S2}, \cdots, Q_{Sz_S})$ and another matrix $\mathbf{N}_S$, of which an element N_{Sij} represents the number of coil turns on the i-*th* stator tooth of the j-*th* phase, it can be shown that magnetic fluxes at the stator teeth, $\mathbf{\Phi}_M$, can be represented in matrix form in terms of the magnetization currents in the 3 phase coils, $\mathbf{I}_{SM}$, as follows :

$$\mathbf{\Phi}_M = \mathbf{D}_S \mathbf{P}_S \mathbf{I}_{SM}, \tag{1}$$

where the matrix $\mathbf{P}_S$ is defined by $\mathbf{P}_S \equiv \mathbf{Q}_S^{-1}\mathbf{N}_S$ and $\mathbf{D}_S$ is a flux influence coefficient matrix an element of which D_{Sij} represents the influence on the i-*th* tooth of the fluxes generated at the j-*th* tooth and is determined from the circuit as shown in Fig. 1(b). Then the voltage $\mathbf{E}_S$ at the three phase coils is induced by the flux change.

In case of no-loaded conditions, relation among the terminal voltage $\mathbf{V}$, induced voltage $\mathbf{E}_S$ and magnetization current $\mathbf{I}_{SM}$ can be derived based upon the electric circuit diagram as shown in Fig. 2(a) by neglecting the current induced in the rotor conductors :

$$\mathbf{V} = \mathbf{R}_S \mathbf{I}_{SM} + \mathbf{E}_S = \left(\mathbf{R}_S + \frac{\mathrm{d}}{\mathrm{dt}}(\mathbf{L}_S)\right)\mathbf{I}_{SM} + \mathbf{L}_S \frac{\mathrm{d}}{\mathrm{dt}}(\mathbf{I}_{SM}), \tag{2}$$

where $\mathbf{R}_S$ is a diagonal matrix representing the resistance of stator coils, $\mathbf{L}_S = \mathbf{N}_S{}^T \mathbf{D}_S \mathbf{P}_S$ represents the self and mutual inductance of the three phase coils in the stator and, hence, is

symmetric.

Electric machines are normally operated under loaded conditions, in which case noise and vibration characteristics are different from those under no-loaded conditions and in the authors' experimental works[2] it was observed that they became more severe. In order to understand why it is so, it is essential to formulate the relations similar to the above under the loaded conditions. The voltage $\mathbf{E}_C$ and the currents $\mathbf{I}_C$ are induced in each conductors of the rotor by the instantaneous slip due to load as shown in Fig. 2(b). In order to calculate the magnetic flux generated by the rotor currents, the equivalent rotor loop consisting of two adjacent conducting bars and two circular arcs of the end rings was modeled as shown in Fig. 2(a). The currents in each rotor loop, $\mathbf{I}_R$, can be obtained from the currents, $\mathbf{I}_C$.

In the same manner as in the stator, defining magnetic reluctance matrix ,$\mathbf{Q}_R$, and $\mathbf{P}_R \equiv \mathbf{Q}_R^{-1}$, the magnetic flux at the stator teeth generated by the rotor current can be written as

$$\mathbf{\Phi}_R = \mathbf{T}_C \mathbf{D}_R \mathbf{P}_R \mathbf{I}_R , \tag{3}$$

where $\mathbf{T}_C$ is a coupling matrix between the stator and rotor teeth an element of which T_{Cij} represents the ratio A_{ij}/A_{Rj} where A_{ij} is the cross sectional area of the i-*th* stator tooth overlapped by the area, A_{Rj}, of j-*th* rotor tooth, $\mathbf{D}_R$ a flux influence coefficient matrix for rotor teeth. Let the currents in the stator induced by the load be $\mathbf{I}_{SL}$, then the magnetic flux $\mathbf{\Phi}_L$ generated at the stator tooth by this current can be calculated by replacing $\mathbf{I}_{SM}$ with $\mathbf{I}_{SL}$ in equation (1). Since the air gap between the stator and the rotor is modeled as in an ideal transformer, the flux change due to the rotor current is canceled out by the one due to the current $\mathbf{I}_{SL}$ induced in the stator. That is,

$$\mathbf{N}_S^{\,T} \frac{d}{dt}(\mathbf{\Phi}_L + \mathbf{\Phi}_R) = \mathbf{0} \tag{4}$$

Therefore, the current $\mathbf{I}_{SL}$ can be calculated from the above relationship. Now, the relationship between the terminal voltages and currents can be written as follows:

$$\mathbf{V} = \mathbf{R}_S(\mathbf{I}_{SM} + \mathbf{I}_{SL}) + \mathbf{L}_S \frac{d}{dt}(\mathbf{I}_{SM}) + \frac{d}{dt}(\mathbf{L}_S)\mathbf{I}_{SM} \tag{5}$$

where it can be seen that the magnetization current is dependent on the resistance of the rotor conductors via the term $\mathbf{R}_S\mathbf{I}_{SL}$.

Applying the formula for radial and tangential force in the air gap of the simple magnetic circuit[7] to the air gap of the induction motor under study, the electromagnetic excitation forces in the radial and tangential directions at the i-*th* stator tooth can be represented for the given geometric configuration and flux distribution at a given instant as follows :

$$F_{Sri} = \sum_{j=1}^{z_R} \frac{B_{ij}^{\,2}}{2\mu_o} A_{ij} , \qquad F_{Sti} = \sum_{j=1}^{z_R} \frac{B_{ij}^{\,2}}{2\mu_o} d_{Si}\left(h_{Sij} - h_{S(i+1)j}\right) , \tag{6}$$

where z_R is the number of rotor teeth, μ_o permeability of the air, h_{Sij} the length of the i-*th* stator slot overlapped by the j-*th* rotor tooth as shown in Fig. 3 and B_{ij} the flux density over A_{ij} due to the currents $\mathbf{I}_{SM}, \mathbf{I}_{SL}$ and $\mathbf{I}_R$.

Variation with time of the above forces can be expressed simply by introducing a given amount of the rotor eccentricity and slot opening width into equations (6). The angular velocity of the rotor which determines the instantaneous slip can be calculated by solving the equation of motion given as follows:

$$r\sum_{j=1}^{Z_R} F_{Stj} - T = J_R \alpha, \qquad (7)$$

where T is the load torque which is in equilibrium with the tangential forces, J_R the mass moment of inertia of the rotor, r the radius of rotor and α the angular acceleration of the rotor.

2.2 Analysis of electromagnetic excitation forces

Variation with time of the electromagnetic excitation force at a stator tooth is shown in Fig. 4. It can be seen that both radial and tangential forces fluctuate mostly at twice the power line frequency($2f_P$ = 120Hz) and that the amplitude of the former is far greater than the latter while increase ratio of the amplitude with loading is smaller in the radial force than in the tangential force.

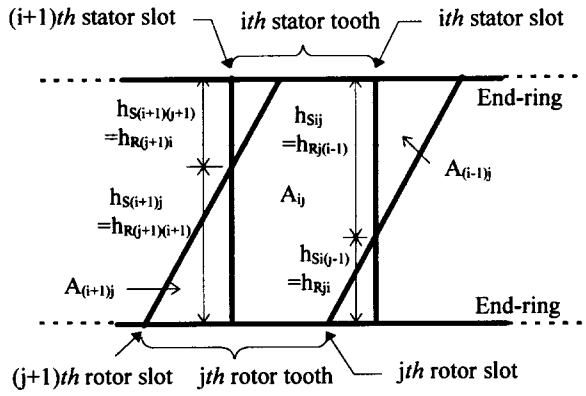

Fig. 3 Geometric configuration of stator and rotor teeth at a given instant

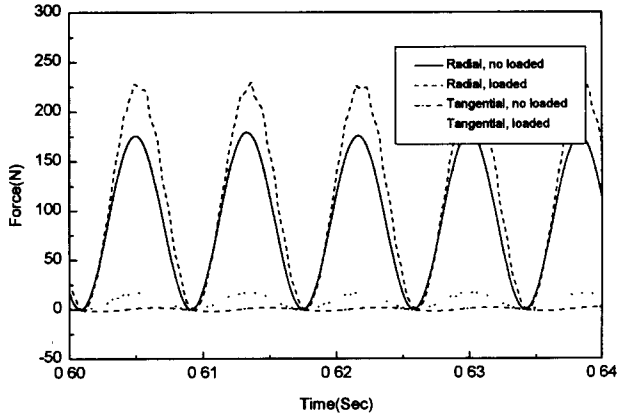

Fig. 4 Radial and tangential components of electromagnetic exciting forces on a stator tooth under no-load and loaded conditions.

Spatial distributions of the radial force are shown in Figs. 5. The radial force can be approximated by Sin(4θ), where θ is the angular position. Distortion of the distribution shape with loading can be explained by the fact that, because spatial variation of the currents in the stator coil and rotor conducting bar becomes more severe with loading, spatial variation of the flux density fluctuation increases accordingly even though flux density fluctuations in each phase of the stator coils are summed up to zero. Noting that the constant component and the Sin(4θ) component of the excitation forces are orthogonal to the oval mode shapes of the structure, which can be described approximately by Sin(2θ) and are most important in this study for a small induction motor, they would not appreciably contribute to the structural vibrations and, therefore, the most meaningful spatial mode of the excitation force would be Sin(2θ) regardless of the temporal frequencies.

Now, the power spectrum of the Sin(2θ) component is shown in Fig. 6 for a given value of the rotor eccentricity and the rotor slot opening under no-loaded and loaded conditions. The results for no rotor eccentricity and no rotor slot opening are shown in Fig. 6(a). The peaks show up with loading at frequencies of 1155Hz($n \times z_R$, where n = 28.9Hz is the rotor speed), 1035 and 1275Hz($n \times z_R \pm 2f_P$). For a chosen value of eccentricity(e=0.1), the power spectrum is shown in Fig. 6(b). The peaks at 1103 and 1338 Hz can be formulated by ($nz_R \pm 2(f_P + n)$). The result for an assumed equivalent width of a rotor slot opening of 1% relative to the slot pitch is plotted in Fig. 6(c). With loading peaks show up at

120Hz($2f_P$) and frequencies($nz_R \pm 2f_P m$) related to the rotor slot passing.

In each case, the overall level increases to some extent with loading as shown in Fig. 6. Many sharp peaks in the measured vibration spectrum[2] coincide with those in Fig. 6(c) and, hence, are considered to have been caused mainly by the rotor slot opening rather than the rotor eccentricity.

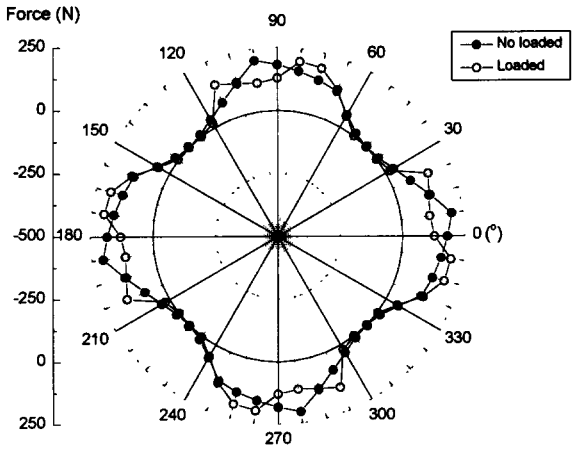

Fig. 5 Distribution of electromagnetic excitation forces in the radial direction over the stator teeth at a given instant

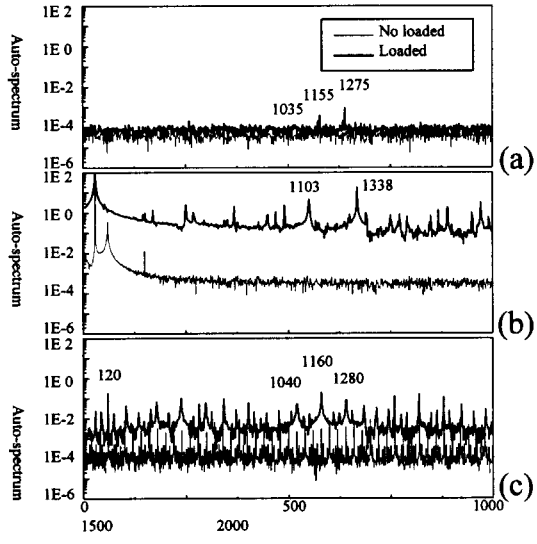

Fig.6 Power spectrum of Sin(2θ) component of the electromagnetic excitation forces

3. Comparison of estimated forces with measurements

The variation of the magnetic flux on a stator tooth was measured by placing a flux-detecting coil around the stator tooth to obtain the Maxwell stress[1] for the purpose of comparison with the computational results. The force signals in the time domain and their power spectrums, predicted by assuming equivalent slot opening width by rather simple criterion using probable flux path[8] and leakage inductance of bridged slot[9] are shown in Figs. 7 and 8 together with the measurements. In order for the magnitudes of the main

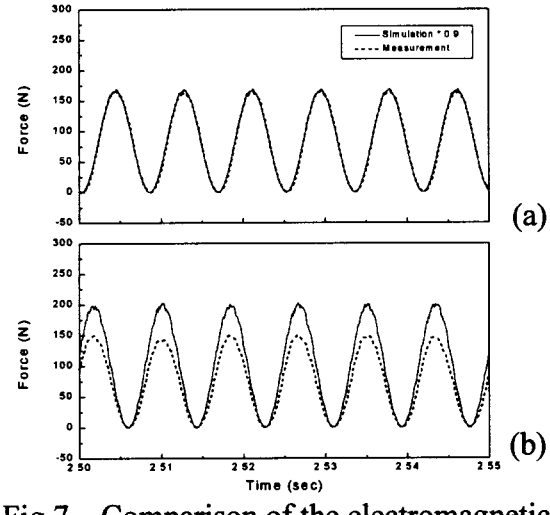

Fig.7 Comparison of the electromagnetic force estimations with measurements

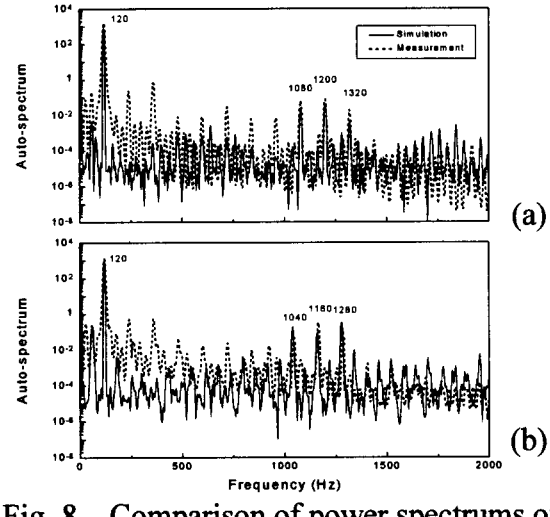

Fig. 8 Comparison of power spectrums of the electromagnetic force estimations with measurements.

flux(120 Hz) under no loaded condition to match each other, a compensation factor 0.9 was multiplied to the results of simulation.

Estimations of the locations of the rotor slot passing related frequencies and their magnitudes coincide well with the measurements. In case of the loaded condition, the magnitude of the main flux is slightly overestimated in simulation as shown in Fig. 7(b). It can be seen by comparison between Fig. 8(a) and (b), however, that the proposed estimation method is capable of describing the tendency of the force increase due to the load at the chosen peak frequencies 1040, 1160, 1280 Hz, and this phenomena agrees relatively well with the measurements.

4. Conclusion

In order to predict the distribution of electromagnetic forces over the stator teeth in an induction motor, simplified analytic equations are formulated in matrix form by employing the modified transformer model. With this model the electromagnetic excitation force at an individual stator tooth can be calculated quantitatively in a very short time.

From this analysis it can be seen that noise and vibration of the induction motor under study is excited mainly by the radial force rather than tangential force, and that with loading the excitation force increases because, even if the total flux linkage at each phase does not change, the flux density changes due to discordance between the positions of the rotor conducting bar and the stator coil. It has been shown that the main source of vibration at many higher harmonics of the rotor rotation is the rotor slot opening rather than the rotor eccentricity because the estimated peak frequencies under the former condition coincide well with the results of the vibration test.

From comparison of predictions of the electromagnetic excitation forces with measurements, it has also been shown that the proposed method is accurate by about 90% under no loaded conditions. But, under the loaded conditions, there are slight discrepancies in the magnitude of the main flux. It may be due to some assumptions which are related with the flux distribution. If these assumptions are improved to be more realistic, more accurate results could be obtained under the loaded conditions as well. The tendency of increasing forces due to the load is described in the frequency range of interest and agrees well with the measurements.

References

[1] F.Kako," Experimental Study on Magnetic Noise of Large Induction Motors," IEEE Trans on PAS,Vol.PAS-102,No.8, pp.2805-2810, August,1983

[2] K.J.Kim,Y.S.Park,D.H.Cho,H.Lee "Experimental Analysis of Noise and Vibration of Integral Horse Power Induction Motors," Internoise, pp105-108, 1995

[3] S,J,Yang, *Low-noise electrical motors*, Clarendon Press, 1981

[4] M.J.DeBortoli,"Effects of Rotor Eccentricity and Parallel Windings on Induction Machine Behavior." IEEE Trans on Magnetics,Vol29,No.2.,pp.1676-1682, 1993

[5] D.H.Cho,K.J,Kim,"Modeling of electro-magnetic excitation forces of an induction motor for vibration and noise analysis", IEE Proc., EPA (Submitted)

[6] An editorial department, *Induction motor*, Ganamsa,1987. (In Korean)

[7] Y.K.Kim, *An illustrated electromagnetics,* Daeyoungsa,1992.(In Korean)

[8] Herbert C.Roters, *Electromagnetic Devices*, John Wiley & Sons, 1955

[9] Paul W. Franklin, *Advanced -Theory and Design of Rotating Electrical Machinery*, The Curators of the University of Missouri,1976

NOMENCLATURE

$\mathbf{D_R}$: Flux influence coefficient matrix of rotor current(z_R x z_R)
$\mathbf{D_S}$: Flux influence coefficient matrix of stator current(z_S x z_S)
$\mathbf{F_{Sr}}$: Electromagnetic excitation force vector at stator teeth in the radial direction (z_S x 1)
$\mathbf{F_{St}}$: Electromagnetic excitation force vector at stator in the tangential direction (z_S x 1)
$\mathbf{I_R}$: Current vector of rotor loop(z_R x 1)
$\mathbf{I_{SM}}$: Current vector of stator coils due to magnetization(3 x 1)
$\mathbf{I_{SL}}$: Current vector of stator coils due to the load(3 x 1)
$\mathbf{L_S}$: Inductance matrix of stator coils defined as $\mathbf{N_S^T D_S P_S}$(3 x 3)
$\mathbf{N_S}$: Matrix of coil turns on stator teeth for 3 phases(z_S x 3)
$\mathbf{P_S}$: Constant matrix defined as $\mathbf{Q_S^{-1} N_S}$ (z_S x z_S) (z_S x 3)
$\mathbf{P_R}$: Constant matrix defined as $\mathbf{Q_R^{-1}}$ (z_R x z_R)
$\mathbf{R_S}$: Diagonal matrix representing resistance of stator coils(3 x 3)
$\mathbf{Q_S}$: Diagonal matrix representing reluctance of stator teeth(z_S x z_S)
$\mathbf{Q_R}$: Diagonal matrix representing reluctance of rotor teeth(z_R x z_R)
$\mathbf{T_C}$: Coupling matrix between stator and rotor tooth an element of which T_{Cij} is given by A_{ij}/A_{Rj} (z_S x z_R)
$\mathbf{\Phi_M}$: Magnetic flux vector of stator teeth due to magnetization current(z_S x 1)
$\mathbf{\Phi_R}$: Magnetic flux vector of stator teeth due to rotor current(z_S x 1)
$\mathbf{\Phi_L}$: Magnetic flux vector of stator teeth due to the load(z_S x 1)